Appl. Phys. B (2016) 122:207
DOI 10.1007/s00340-016-6481-1

Applied Physics B
Lasers and Optics

Calculation of electron binding energies of Na_{55}^- clusters

Armen Melikyan[1] · Hayk Minassian[2] · Valeri G. Grigoryan[3] · Michael Springborg[3,4]

Received: 12 August 2015 / Accepted: 25 June 2016 / Published online: 12 July 2016

Abstract Within the frame of the one-electron approximation, we calculate the electron binding energies of the Na_{55}^- cluster which allows for the identification of the icosahedral structure of the cluster through comparison with experimental photoelectron spectroscopy data. The surface of the icosahedral cluster is represented as a slightly deformed spherical surface, and the corresponding splitting of the energy levels caused by this symmetry reduction is calculated. Subsequently, we demonstrate that the calculated energies of photoelectrons agree very well with the experimental values. This gives an unambiguous demonstration of the role of the cluster structure in photoelectron spectra, whereas electronic shell filling effects are less important.

1 Introduction

Currently, metal clusters (MC) are intensively studied both experimentally and theoretically not only because of their scientifically interesting properties as systems intermediate between small molecules and macroscopic clusters, but also in connection with possible applications in the design of small-scale electronic and optoelectronic devices [1–4].

Experimental study of the electronic structure of MC often applies one of the following two approaches: (a) investigation of photoelectron spectra (PES) or (b) investigation of surface plasmon (SP) spectra. With the first method, an incident wave with photon energy exceeding the work function causes direct photoionization [5, 6], whereas in the second case, radiation with relatively long wavelength excites collective electron oscillations, i.e., SPs with resonance frequencies strongly depending on the shape and size of the MC [7]. While the PES provide information on the electronic structure directly, the SP spectra allow extracting aspect ratios that in turn determine the electronic structure of MC [8, 9].

Earlier, it has been shown that there exist simple analytical methods that can be used in relating the parameters describing the cluster shape with the characteristic energies of SP oscillations. In Ref. [7] a formula linking SP frequencies with the depolarization factors for spheroidal clusters was presented. For particles with small and arbitrary deviations from the spherical shape, the dependence of the SP spectrum on geometrical parameters was treated more recently [8]. Both of these two studies demonstrated a good agreement with existing experimental information.

Theoretically, PES can be calculated using various, more or less accurate, methods based on density-functional theory (DFT) [10]. Many, highly accurate, methods taking the full geometric arrangement of the atoms as well as the electronic properties into account exist, but often less accurate phenomenological methods are useful in rationalizing the properties of the MC. Thus, within the frame of the jellium model [7, 11], DFT was utilized to reveal the electronic shell structure in relatively small MCs. It turned out, however, that, e.g., for Na_N clusters with $N \geq 55$, the

✉ Valeri G. Grigoryan
vg.grigoryan@mx.uni-saarland.de

[1] Russian-Armenian (Slavonic) State University, 123 Hovsep Emin Street, 0051 Yerevan, Armenia

[2] A. Alikhanian National Scientific Laboratory, 2 Alikhanian Br. Str., 0036 Yerevan, Armenia

[3] Physical and Theoretical Chemistry, University of Saarland, 66123 Saarbrücken, Germany

[4] School of Materials Science and Engineering and Tianjin Key Laboratory of Composites and Functional Materials, Tianjin University, Weijin Road, No. 92, Tianjin 300072, China

electronic states are mostly determined by the geometry of the MC. Particularly, it has been found that for smaller particles cluster stability is dominated by electron shell closing effects, whereas that of the larger ones is governed by geometrical packing effects [6]. This circumstance may also imply that the electronic shell structure is smeared out in larger clusters. Thus, for the latter, the influence of geometrical packing effects on the electron spectrum needs to be thoroughly taken into account in order to be able to interpret experimental data on PES.

It is well known that the cluster geometry is determined by the requirement that it is the global minimum of the potential energy surface [12]. In particular, earlier studies (e.g., [5]) show that MC with $N = 55$, 147, 309 corresponding to 3, 4, and 5 complete shells of atoms clearly favor the icosahedral shape. Thus, for Na_N clusters with the above-mentioned number of atoms, the measured PES are in good agreement with the DOS calculated with DFT methods for Mackay icosahedrons [5, 6].

In the present work, the energies of electronic states in an ideal icosahedral cluster anion with $N = 55$ atoms are calculated using a one-electron approximation. The purpose is to study the influence of geometrical packing effects on the results of PES experiments [5, 6]. In our approach, the collective effect of electrons in the clusters with $N \geq 55$ is neglected, which means that the electronic spectrum in these MC is assumed to be determined mainly by the shape of the surface. We emphasize that the system of interest is one for which geometrical packing effects dominate over electronic shell filling effects and one for which deviations from spherical symmetry are sufficiently small to be treated using perturbation theory.

We describe an ideal icosahedral cluster in the spirit of the study in Ref. [8] with the difference that instead of solving a boundary problem for the Laplace equation we solve the boundary problem for the Schrödinger equation. We show that the surface of the icosahedral cluster can be presented as a slightly deformed spherical surface. With this approach, the structure of the energy levels in an icosahedral quantum well is interpreted in terms of the symmetry reduction due to the small deformation of a sphere. It is clear that the icosahedral deformation leads to a splitting of the corresponding energy levels compared with the case of the spherical quantum well. We show that, within a one-electron approximation, the peak positions of the photoelectron spectra of the Na_{55}^- cluster are in good agreement with experimental data and DFT calculations. Thus, we demonstrate that it is possible to use photoelectron spectra to determine the structure of non-spherical clusters, also for those clusters for which geometrical packing effects are dominating in dictating stability.

2 Approach

Recently, the results of DFT simulations of the density of states (DOS) of sodium cluster anions in the size ranges 39–350 atoms [5] and 13–80 atoms [6] were presented. Here, we use a more phenomenological approach for a Na_{55} cluster, which is of great interest as it is the simplest icosahedral structure for which the electron energy spectrum is assumed to be determined by the geometrical packing effects. We are convinced that our approach is practical also for other systems and/or cluster sizes, in particular because the computational requirements do not grow strongly with cluster size, making it an interesting alternative for larger clusters.

Assuming in clusters with $N \geq 55$ that their stability is governed by geometric packing effects, rather than electronic shell closing effects, we shall apply a single-electron description (i.e., a non-interacting electron approximation).

As reference (zeroth approximation), we use the energies of the electronic levels as determined for the infinite spherical well. The energy spectrum of an electron in such a well is described in detail in Ref. [13]. The distribution of particles over the levels corresponding to the lowest value of energy of a system of 55 non-interacting electrons has, accordingly, the following form. The states with radial quantum number $n = 1$ and orbital quantum number $l = 0$, 1, 2, and 3 are fully populated by in total 32 electrons. The next 8 electrons occupy the states with $n = 2$ and $l = 0$, 1. The remaining 15 electrons occupy the states with the quantum numbers $n = 1$, $l = 4$, for which 3 orbitals remain unoccupied. As calculations show, the energetic ordering of these levels is not changed when passing to a spherical well of finite depth. However, as our calculations show, the model of a spherical well of finite depth does not provide good agreement with the photoionization data. Note that the simplest way for describing deviations from spherical shape is obtained by treating the clusters as being a spheroid with small eccentricity. In particular, this approach allows estimating the splitting of SP frequencies caused by the lifting of the degeneracy (see, e.g., Ref. [7]). This approach, however, turns out to be inadequate when attempting to describe icosahedral clusters since it does not account for the specific symmetry that determines the character of the electron level splitting.

Thus, it is clear that it is not a good approximation to treat an ideal icosahedron as being close to a sphere or spheroid. However, as we demonstrate in Sect. 3, within the framework of perturbation theory, we can determine the effects of a non-spherical shape on the degeneracies of the electronic levels. We mention that it is possible to describe the shape of an icosahedron as a weakly deformed sphere so that all symmetries are taken into account. Indeed, the

radius of a circumscribing sphere (one that touches the icosahedron at all 12 vertices) is $r_u = 0.95a$, the radius of an inscribed sphere (tangent to each of the icosahedron's 20 faces) is $r_i = 0.76a$, and the midradius, which touches the middle of each of the 30 edges, is $r_m = 0.81a$, where a is the length of the icosahedron edge. Using these radii, we introduce aspect ratios of the regular icosahedron as follows: $\zeta_1 = r_u/r_m$ and $\zeta_2 = r_u/r_i$ that take the values 1.17 and 1.25, respectively. As will be shown below, the deviations of those numbers from the value 1 for a perfect sphere have strong impacts on the electron spectrum of the cluster.

To exploit those deviations from spherical shape, we introduce an approximate analytical description of the icosahedral surface that differs from an ideal one by having smooth edges and vertices. In spherical coordinates r, θ, and φ, the shape of a non-spherical cluster can be presented by

$$r(\theta,\varphi) = R[1 + F(\theta,\varphi)], \tag{1}$$

where the deviation of the function $F(\theta,\varphi)$ from a constant describes the deviation from spherical shape, and the parameter R will be defined below. It is easy to verify that a surface possessing icosahedral symmetry with smooth edges and vertices can be presented by the following function (see "Appendix" section)

$$F(\theta,\varphi) = c\,[1 - a^2\cos^2(\theta)]^{-4} + \sum_{m=1}^{5} c\left\{1 - a^2\left[b\cos(\theta) + \sqrt{1-b^2}\sin(\theta)\cos\left(\varphi - \frac{2\pi}{5}(m-1)\right)\right]^2\right\}^{-4}, \tag{2}$$

where a and c are fitting parameters and $b = \cos(2\pi/5)[1 - \cos(2\pi/5)]^{-1}$. It turns out that the best fit to the icosahedral shape is reached if, in Eq. (2), the parameters take the values $a = 0.67$ and $c = 1$. The corresponding aspect ratios for those values of a and c are $\zeta_1 = 1.20$ and $\zeta_2 = 1.23$ that differ from the exact values of 1.17 and 1.25 by just 3 %.

Expression (1), after performing an identical transformation, can be presented in the following convenient form

$$r(\theta,\varphi) = \langle r(\theta,\varphi)\rangle[1 + f(\theta,\varphi)], \tag{3}$$

where

$$f(\theta,\varphi) = \frac{F(\theta,\varphi) - \langle F(\theta,\varphi)\rangle}{1 + \langle F(\theta,\varphi)\rangle}, \qquad \langle r(\theta,\varphi)\rangle = R[\,1 + \langle F(\theta,\varphi)\rangle\,]. \tag{4}$$

In (3) and (4), the brackets $\langle\cdots\rangle$ represent averaging over the solid angle. Expressions (3) and (4) allow introducing the mean radius that can be considered as the definition of the parameter R in (1). In fact, the average value $r_{av} = \langle r(\theta,\varphi)\rangle$ represents the radius of the sphere to which the icosahedron is fitted.

Thus, although our model is not able to describe sharp edges and vertices rigorously, this approach allows not only to preserve the icosahedral symmetry but also by fitting the parameters to come very close to the ideal values of aspect ratios ζ_1 and ζ_2.

In the next sections, we shall calculate the energy spectrum of an electron in the quantum well of the form described by (1)–(4).

3 Energy level splitting in icosahedral quantum well and comparison with experiment

We consider a cluster with a shape described by Eqs. (2)–(4) in which, because of the reduction in spherical symmetry, the degeneracies of the energy levels are lowered compared with the spherical case. When attempting to determine the energy spectrum of the electrons, one needs parameters of the shape and depth of the icosahedral potential well.

First, we determine the parameters of an icosahedral potential well with depth V_0 assuming for simplicity that the potential across the boundary changes abruptly from $-V_0$ to zero. To determine values for the parameters r_{av} [see (4)] and V_0, we use experimental data on the PES for the sodium anion cluster Na_{55}^- [see Fig. 2 of [5] which we will refer to as Fig. (Na_{55}^-)].

Due to the icosahedral deformation from a sphere, the levels $n = 1$, $l = 4$ are split into two levels, as will be shown below. We assume that the second and the third peaks from the right in Fig. (Na_{55}^-) correspond to this splitting. Therefore, the minimum (between these two peaks) located at the energy $E_{1,4} = 2.22$ eV corresponds

to the degenerate state $n = 1$, $l = 4$ for the spherical well. This statement is justified by the experimental fact that there are no states with the energy 2.22 eV [see Fig. (Na_{55}^-)].

The peak at $E_{2,1} = 2.64$ eV in Fig. (Na_{55}^-) will be ascribed to the level $n = 2$, $l = 1$ for the spherical well which, as will be shown below, is not split for the icosahedral symmetry and, therefore, remains occupied.

Next we shall show that knowledge of these two binding energies for the states $n = 1$, $l = 4$ and $n = 2$, $l = 1$ makes it possible to determine the values of $r_{\rm av}$ and V_0. For this purpose, we write the equation determining the spectrum of a particle in the spherical potential well of finite depth, $-V_0$ [13]

$$ik\frac{h_l^{(1)'}(ikr_{\rm av})}{h_l^{(1)}(ikr_{\rm av})} = q\frac{j_l'(qr_{\rm av})}{j_l(qr_{\rm av})}, \tag{5}$$

where j_l is a spherical Bessel function of order l, $h_l^{(1)}$ is a spherical Hankel function of imaginary argument of order l, and the primes denote derivatives. The variables k and q are defined as $k = \sqrt{2\mu E/\hbar^2}$, $q = \sqrt{2\mu(V_0 - E)/\hbar^2}$, where μ and E are the mass of the particle and its binding energy, respectively.

We denote the first root of Eq. (5) for $l = 4$ as $k_{1,4}$ and the second root of the same equation for $l = 1$ as $k_{2,1}$ for which the corresponding energies are $E_{1,4} = \hbar^2 k_{1,4}^2/2\mu$, $E_{2,1} = \hbar^2 k_{2,1}^2/2\mu$. Since we have from experimental data [5] $E_{1,4} = 2.22$ eV and $E_{2,1} = 2.64$ eV this gives $k_{2,1}^2/k_{1,4}^2 = 1.19$. Note that depending on V_0, the values of k and q must satisfy $k^2 + q^2 = 2\mu V_0/\hbar^2$. Next, we choose the parameter $\eta = r_{\rm av}\sqrt{2\mu V_0/\hbar^2}$ so that the equality $k_{2,1}^2/k_{1,4}^2 = 1.19$ is satisfied. The corresponding fitting procedure gives $\eta_{\rm fit} = 9.25$. Together with $\eta_{\rm fit}$, we then obtain values for the solutions to Eq. (5), i.e., $k_{2,1}r_{\rm av} = 6.17$ and $k_{1,4}r_{\rm av} = 5.66$. Moreover, from the relation $k_{1,4}^2/\eta_{\rm fit}^2 = |E_{1,4}|/V_0$ we find for the well depth $V_0 = 5.88$ eV that leads to $r_{\rm av} = 7.45$ Å.

Finally, we identify the two peaks in Fig. (Na_{55}^-) located at 2.90 and 3.28 eV as originating from the state $n = 1$, $l = 3$ in the spherical well but here being split due to the icosahedral deformation. Below we shall calculate the splittings of the levels $n = 1$, $l = 4$ and $n = 1$, $l = 3$, thereby exploiting our concept of small deviations from spherical shape.

Weakly bound electrons that are responsible for the rightmost peak at 1.8 eV of the experimental data of Fig. (Na_{55}^-) are at higher energy levels of the potential well, and hence, they spend in their motion more of their time near the surface of the cluster in comparison with electrons with higher binding energy. Accordingly, the energy levels of these electrons are more sensitive to the fine details of the cluster surface than electrons with higher binding energy. Perhaps this is one of the reasons why our study, which approximately describes the structure of the icosahedral cluster, does not work properly for the weakly bound electrons that are responsible for the peak of 1.8 eV.

To determine the energy levels of Na_{55}^- and compare those with the experimental PES of this system, we seek the solutions to the Schrödinger equation inside and outside of the well which is supposed to have the following form

$$\Psi_{\rm in} = \sum_{lm} a_{lm}\, j_l(qr)\, Y_{lm}(\theta,\varphi) \qquad \Psi_{\rm out} = \sum_{lm} b_{lm}\, h_l(ikr)\, Y_{lm}(\theta,\varphi), \tag{6}$$

where $Y_{lm}(\theta,\varphi)$ is a spherical harmonic. The coefficients a_{lm} and b_{lm} in (6) are determined from the boundary conditions for the wave function of the particle in the icosahedral well (2)–(4),

$$\begin{aligned}
&\sum_{lm} a_{lm}\, j_l[qr(\theta,\varphi)]\, Y_{lm}(\theta,\varphi) = \sum_{lm} b_{lm}\, h_l[ikr(\theta,\varphi)]\, Y_{lm}(\theta,\varphi),\\
&\sum_{lm} a_{lm}\left\{qj_l'[qr(\theta,\varphi)]Y_{lm}(\theta,\varphi) - j_l[qr(\theta,\varphi)]r_{\rm av}\nabla f(\theta,\varphi)\nabla Y_{lm}(\theta,\varphi)\right\}\\
&= \sum_{lm} b_{lm}\left\{ikh_l'[ikr(\theta,\varphi)]Y_{lm}(\theta,\varphi) - h_l[ikr(\theta,\varphi)]r_{\rm av}\nabla f(\theta,\varphi)\nabla Y_{lm}(\theta,\varphi)\right\}.
\end{aligned} \tag{7}$$

Table 1 Calculated binding energy (in eV) of the different quantum levels in Na_{55}^- cluster modeled through the spherical (second column) and icosahedral (third column) finite wells

States in a spherical well	Finite spherical well	Finite icosahedral well	Experimental values
$n = 1,\ l = 4$	2.22	Split: 2.07 and 2.37	2.05 and 2.35
$n = 2,\ l = 1$	2.64	Unsplit: 2.64	2.64
$n = 1,\ l = 3$	3.20	Split: 3.04 and 3.32	2.90 and 3.28

The fourth column displays the corresponding experimental data

In the spirit of [8], we apply the concept of weak deviations from spherical symmetry to the boundary conditions (7). Then the angular momentum in Eq. (7) is no longer a good quantum number and the $(2l + 1)$-fold degeneracy is lowered. However, for a sufficiently small f, as will be shown below, the splitting is smaller than the separation of energy levels with different l. Thus, we can apply a zero-order approximation of perturbation theory to (7) keeping only terms to first order in $f(\theta, \varphi)$ [14] which results in

$$\begin{aligned} &j_l'(q_0 r_{\rm av})\Delta q a_{lm} + j_l'(q_0 r_{\rm av}) q_0 \sum_{m'} \langle lm|f(\theta,\varphi)|lm'\rangle a_{lm'} \\ &\quad = i h_l'(ik_0 r_{\rm av})\Delta k b_{lm} + i h_l'(ik_0 r_{\rm av}) k_0 \sum_{m'} \langle lm|f(\theta,\varphi)|lm'\rangle b_{lm'} \end{aligned} \tag{8}$$

and

$$\begin{aligned} &\left[j_l'(q_0 r_{\rm av}) + q_0 r_{\rm av} j_l''(q_0 r_{\rm av})\right]\Delta q a_{lm} \\ &\quad + q_0^2 r_{\rm av} j_l''(q_0 r_{\rm av}) \sum_{m'} \langle lm|f(\theta,\varphi)|lm'\rangle a_{lm'} \\ &\quad = \left[i h_l'(ik_0 r_{\rm av}) - k_0 r_{\rm av} h_l''(ik_0 r_{\rm av})\right]\Delta k b_{lm} \\ &\qquad - k_0^2 r_{\rm av} h_l''(ik_0 r_{\rm av}) \sum_{m'} \langle lm|f(\theta,\varphi)|lm'\rangle b_{lm'} \end{aligned} \tag{9}$$

where $\langle lm|f(\theta,\varphi)|\,lm'\rangle$ is a matrix element for the function $f(\theta,\varphi)$ between spherical harmonics. Moreover, k_0 and q_0 are the roots of the equation (5) for fixed l, $\Delta k = k - k_0$, and $\Delta q = q - q_0$. Then, writing in (8) and (9) Δk and Δq as $\Delta k = \mu(|E| - |E_0|)/\hbar^2 k_0$ and $\Delta q = \mu(|E| - |E_0|)/\hbar^2 q_0$ we arrive at a homogeneous set of equations for a_{lm} and b_{lm}. The condition of the existence of non-trivial solutions to this set gives the sought values for the energy level splitting $\Delta E = |E| - |E_0|$.

The numerical calculations of this determinant equation show that the icosahedral deformation of a spherical cluster does not lift the degeneracy of s, p, and d energy levels for any n corresponding to the spherical well. In particular, the level $n = 2$, $l = 1$, as mentioned above, does not split and remains occupied in agreement with the experimental data.

Our further calculations show that contrary to the case for the s, p, and d levels, f and g states for the same $n = 1$ each split into two sublevels. Using the values determined above, i.e., $V_0 = 5.88$ eV and $r_{\rm av} = 7.45$ Å, we obtain the following values for the splitting of f and g states correspondingly: $\Delta E_{1,4} \approx 0.30$ eV and $\Delta E_{1,3} \approx 0.28$ eV. The positions of the peaks at 2.35 eV and 2.05 eV, originating from the splitting of the level with $n = 1$, $l = 4$ in the spherical well, are in very good agreement with experimental data. In Table 1, we summarize the obtained energies together with the assigned quantum numbers for the Na_{55}^- cluster modeled both through the spherical and the icosahedral finite wells. The last column of the table shows the corresponding experimental data. As given in Table 1, the obtained values for the binding energies of the five states in the finite icosahedral cluster in the range of $2.0 - 3.3$ eV fit well with the experimental peaks as well as with the DFT calculations [see black and red curves of Fig. (Na_{55}^-)].

The calculation for finite spherical well based on Eq. (5) predicts also the existence of a level with a binding energy of 3.2 eV. The most probable candidate for this position is the level corresponding to $n = 1$, $l = 3$ in the spherical well that is depopulated because of the splitting caused by icosahedral deformation. Indeed, there is a minimum in the PES at 3.1 eV in the experimental plot in Fig. (Na_{55}^-). Our calculated value of the splitting, ≈ 0.28 eV, agrees well with the experimental data. Note that the calculated splittings of the states $n = 1$, $l = 4$ and $n = 1$, $l = 3$ differ by symmetry. Namely the first one is symmetric (± 0.15 eV), whereas the second one is asymmetric (-0.16 and $+0.12$ eV). Further, in the range of binding energies 3.0–3.3 eV there are several other peaks [see Fig. (Na_{55}^-)] that are strongly broadened due to the short lifetime of holes in energetically deeper states.

So far, it has not been possible to explain the weakly observed peaks at 2.5 and 2.8 eV, neither using geometrical packing effects (this study) nor using electron shell closing effects [5]. However, a competitive channel of photoionization via Auger transitions could be responsible for those peaks. Particularly, our analysis of the energy spectrum of electrons in an icosahedral well shows that the level with $n = 1$, $l = 1$ can be depopulated by virtual absorption of a 4 eV photon, resulting in a hole, that subsequently through an Auger process can be occupied by an electron from one of the two split sublevels of the state $n = 1$, $l = 4$. The energy released in this process could be transferred to another electron in these sublevels ultimately resulting

in ionization. That this suggestion is realistic can be seen from the energy separation of the levels with binding energies 2.5 and 2.8 eV that equals the difference of the binding energies of the $n = 1$, $l = 4$ sublevels.

Thus, we have shown that geometrical packing effects provide good agreement with the experiment data for Na_{55}^-. Since the measured PES are in good agreement with the DOS calculated for Mackay icosahedrons[5, 6] in the framework of DFT as well, we conclude that in the DFT calculations the electron correlation effects are not dominating.

4 Conclusion

Using a more phenomenological approach, we have calculated the energy levels of electrons in an icosahedral Na_{55}^- cluster within a one-electron approximation. The shape of the icosahedral cluster is described as a slightly deformed spherical shape, and the corresponding energy splittings of the energy levels caused by this symmetry reduction are calculated. We show that the calculated peak positions of the photoelectron spectra of the Na_{55}^- cluster are in good agreement with experimental data and DFT calculations. Ultimately this suggests that the photoelectron spectra can also be used in obtaining detailed information on the overall shape of larger clusters for which more accurate calculations become prohibitive.

Acknowledgments This work was supported by the State Committee of Science of Ministry of Education and Science of the Republic of Armenia in frame of the research Project #SCS-13-1C353 and by the Deutsche Forschungsgemeinschaft (DFG) through Project No. SP 439/34-1.

Appendix

Expression (2) for $F(\theta, \varphi)$ is based on the following arguments. Let $\vec{n}_k$ be a unit vector directed from the center of a polyhedron to its kth vertex. We introduce the function $g(\theta, \varphi)$

$$g(\theta, \varphi) = \frac{1}{[1 - a^2(\vec{n}\vec{n}_k)^m]^n}, \tag{10}$$

where $\vec{n} = \vec{r}/r$, $\vec{r}$ is radius vector and $a^2 < 1$. The function (10) is chosen so that it increases sharply when $\vec{n}$ approaches $\vec{n}_k$. Correspondingly, the sum

$$\sum_{k=1}^{N} \frac{1}{[1 - a^2(\vec{n}\vec{n}_k)^m]^n} \tag{11}$$

has maxima for all directions $\vec{n}$ coinciding with some $\vec{n}_k$. In (11), N is the number of vertices which in the case of an icosahedron is 12. The magnitudes of a and the exponents

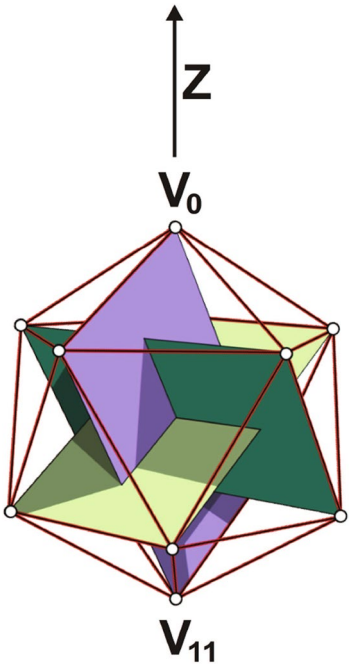

Fig. 1 *Icosahedron* vertices form three orthogonal *golden rectangles* (https://en.wikipedia.org/wiki/Regular_icosahedron)

m and n in the denominator of (11) are chosen so that the aspect ratios of the surface described by the function (11) are close to those of icosahedron. The fitting procedure leads to $a = 0.67$, $m = 2$, $n = 4$.

The Z-axis in Fig. 1 is placed along the straight line connecting two opposite vertices V_0 and V_{11}. We use an index 0 for the upper vertex of the icosahedron and an index 11 for the lowest one. Thus, we have $\vec{n}_{11} = -\vec{n}_0$. Below vertex number 0 (V_0), there are five vertices forming a pentagon (see Fig. 2) centered at O_1 with side a (being the side of the icosahedron) and the radius r of the circumcircle. Figure 2 shows that $a = 2r\sin(\pi/5)$ or

$$a = \sqrt{2}r\sqrt{1 - \cos(2\pi/5)}. \tag{12}$$

In Fig. 3, O is the center of the icosahedron, V_0 and V_1 denote the vertices, $OV_0 = OV_1 = R$, R is the radius of the circumscribing sphere of the icosahedron, and $O_1V_1 = r$ is the circumcircle of the pentagon, respectively. Denoting O_1V_0 as h, we write $a^2 - r^2 = h^2$ and $r^2 + (\,OO_{\,1})^2 = R^2$. Combining with Eq. (12), we obtain

$$\frac{OO_{\,1}}{R} = \frac{\cos(2\pi/5)}{1 - \cos(2\pi/5)}. \tag{13}$$

Note that OO_1/R is the projection of the unit vector $\vec{n}_1$ along the Z-axis, and r/R is the projection of the same vector along the X-axis, which coincides with the direction of the vector O_1V_1.

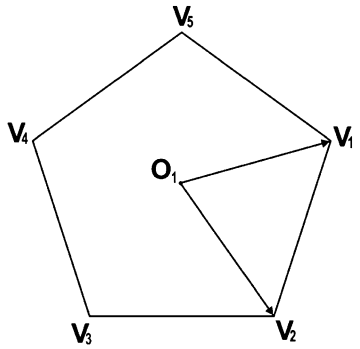

Fig. 2 Five vertices forming *pentagon* centered at O_1

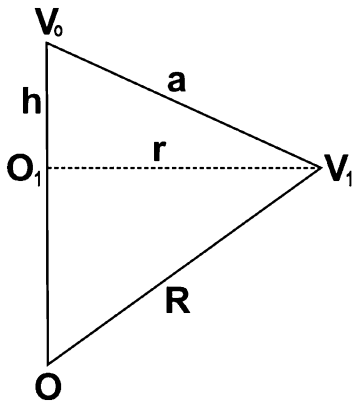

Fig. 3 Section of an *icosahedron* with the center at O and the two adjacent vertices V_0 and V_1

Another pentagon located in Fig. 1 further below is rotated with respect to the one just discussed by the angle $\pi/5$, and, thus, the whole system of the vertices possesses central symmetry. This means that the 12 unit vectors form two groups (six vectors in each group) so that every unit vector from the first group has its opposite one in the second group: $\vec{n}_k$ ($k = 0, 1, 2, 3, 4, 5$) and $-\vec{n}_k$ ($k = 0, 1, 2, 3, 4, 5$). Now, using Fig. 3 we can write the components of the first six unit vectors as

$$\begin{aligned}
\vec{n}_0 &= (0, 0, 1),\\
\vec{n}_1 &= \left(\sqrt{1-b^2}, 0, b\right),\\
\vec{n}_2 &= \left(\sqrt{1-b^2}\cos(2\pi/5), \sqrt{1-b^2}\sin(2\pi/5), b\right),\\
\vec{n}_3 &= \left(\sqrt{1-b^2}\cos(4\pi/5), \sqrt{1-b^2}\sin(4\pi/5), b\right),\\
\vec{n}_4 &= \left(\sqrt{1-b^2}\cos(6\pi/5), \sqrt{1-b^2}\sin(6\pi/5), b\right),\\
\vec{n}_5 &= \left(\sqrt{1-b^2}\cos(8\pi/5), \sqrt{1-b^2}\sin(8\pi/5), b\right),
\end{aligned} \tag{14}$$

where $b = \frac{\cos(2\pi/5)}{1-\cos(2\pi/5)}$. Using (14) one can calculate $\vec{n}\vec{n}_k$ in (10) and (11). For example, the scalar product $\vec{n}_4\vec{n}_k$ can be expressed as

$$\begin{aligned}
\vec{n}_4\vec{n}_k = {} & b\cos(\theta) + \sqrt{1-b^2}\\
& \sin(\theta)[\cos(\varphi)\cos(4\pi/5) + \sin(\varphi)\sin(4\pi/5)]
\end{aligned} \tag{15}$$

Substituting all the products $\vec{n}\vec{n}_k$ into (11), we obtain Eq. (2) of the main text.

References

1. D.L. Andrews, Z. Gaburro (eds.), *Frontiers in Surface Nanophotonics, Principles and Applications* (Springer, New York, 2007)
2. M.L. Brongersma, P.G. Kik (eds.), *Surface Plasmon Nanophotonics* (Springer, Dordrecht, 2007)
3. F. Träger, Special issue: optical properties of nanoparticles. Appl. Phys. B Lasers Opt. **73**, 291–429 (2001)
4. S.M. Morton, D.W. Silverstein, L. Jensen, Chem. Rev. **111**, 3962 (2011)
5. O. Kostko, B. Huber, M. Moseler, B. von Issendorff, Phys. Rev. Lett. **98**, 043401 (2007)
6. A. Aguado, O. Kostko, J. Chem. Phys. **134**, 164304 (2011)
7. W.D. Knight, K. Clemenger, W.A. de Heer, W.A. Saunders, M.Y. Chou, M.L. Cohen, Phys. Rev. Lett. **52**, 2141 (1984)
8. A. Melikyan, H. Minassian, V.G. Grigoryan, M. Springborg, Appl. Phys. B **112**, 177 (2013)
9. V.G. Grigoryan, M. Springborg, H. Minassian, A. Melikyan, Comp. Theor. Chem. **1021**, 197 (2013)
10. P. Hohenberg, W. Kohn, Phys. Rev. **136**, B864 (1964)
11. W. Ekardt, Phys. Rev. B **29**, 1558 (1984)
12. F. Baletto, R. Ferrando, Rev. Mod. Phys. **77**, 371 (2005)
13. S. Flügge, *Practical Quantum Mechanics* (Springer, Berlin, 1999)
14. L.D. Landau, E.M. Lifshitz, *Quantum Mechanics: Non-relativistic Theory* (Pergamon Press, Oxford, 1977)